ISSN 1068-7998, Russian Aeronautics, 2019, Vol. 62, No. 4, pp. 633–642. © Allerton Press, Inc., 2019.
Russian Text © The Author(s), 2019, published in Izvestiya Vysshikh Uchebnykh Zavedenii, Aviatsionnaya Tekhnika, 2019, No. 4, pp. 98–106.

AERO- AND GAS-DYNAMICS OF FLIGHT VEHICLES AND THEIR ENGINES

Application of the Implicit MacCormack Scheme for Computation of Supersonic Turbulent Jets Using the Parabolized Navier–Stokes Equations

A. M. Molchanov[a], A. S. Myakochin[a,*], I. N. Borovik[a], and A. S. Tushkanov[a]

[a]*Moscow Aviation Institute (National Research University), Volokolamskoe sh. 4, Moscow, 125993 Russia*

**e-mail: myakochinas@mai.ru*

Received February 18, 2019; in final form, October 3, 2019

Abstract—An effective unconditionally stable numerical method for solving equations describing the flow of supersonic turbulent jets is developed. The method does not require the inversion of block tridiagonal systems of algebraic equations. The results obtained according to this method are in fairly close agreement with the calculations results on the basis of other methods and experimental data.

DOI: 10.3103/S1068799819040147

Keywords: supersonic jets, turbulence, compressibility, Navier–Stokes equations, parabolization.

In recent decades, significant progress has been made in mathematical modeling of supersonic gas flows. The problem is solved on the basis of the complete Navier–Stokes equations [1, 2] as well as using the simplified (parabolized) Navier–Stokes equations [3–6].

Explicit numerical methods are usually used to calculate jets based on the parabolized Navier–Stokes equations. The main disadvantage of such schemes is the limitation of size of the longitudinal integration step, which can lead to a significant increase in computation time. In using implicit schemes [6], it becomes necessary to construct very complex matrices and solve them. This is true especially for flows with subsonic regions.

In the early 1980s, MacCormack [7] proposed an effective implicit method for solving the complete unsteady Navier–Stokes equations. The main advantages of this method are unconditional stability and no need to solve equations with block tridiagonal matrices.

This paper presents a modification of the implicit MacCormack method that is applicable for solving the parabolized Navier–Stokes equations. Particular attention is paid to modeling turbulence in supersonic flows.

The equations of flow of a turbulent gas mixture can be obtained by a formal averaging of the unsteady Navier–Stokes equations. In this paper, two methods of division of variables into the average and fluctuating components are used:

1) $p = \overline{p} + p'$, where the line means the ensemble averaging;

2) $u = \tilde{u} + u''$, where $\tilde{u} = \overline{\rho u} / \overline{\rho}$ is the averaging by density as a weighting factor.

The equations for a high Reynolds number axisymmetric jet, when the chemistry is frozen, are given below

$$\frac{\partial}{\partial x}\left(\overline{\rho}\tilde{u}\right) + \frac{\partial}{\partial y}\left(\overline{\rho}\tilde{v}\right) + \frac{\overline{\rho}\tilde{v}}{y} = 0\,; \tag{1}$$

$$\overline{\rho}\tilde{u}\frac{\partial \tilde{u}}{\partial x} + \overline{\rho}\tilde{v}\frac{\partial \tilde{u}}{\partial y} = -\frac{\partial \overline{p}}{\partial x} - \frac{\partial}{\partial x}\left(\overline{\rho}\widetilde{u''^2}\right) - \frac{\partial}{\partial y}\left(\overline{\rho}\widetilde{u''v''}\right) - \frac{\overline{\rho}\widetilde{u''v''}}{y}\,; \tag{2}$$

$$\bar{\rho}\tilde{u}\frac{\partial\tilde{v}}{\partial x}+\bar{\rho}\tilde{v}\frac{\partial\tilde{v}}{\partial y}=-\frac{\partial\bar{p}}{\partial y}-\frac{\partial}{\partial x}\left(\bar{\rho}\widetilde{u''v''}\right)-\frac{\partial}{\partial y}\left(\bar{\rho}\widetilde{v''^2}\right)-\frac{\bar{\rho}\left(\widetilde{v''^2}-\widetilde{w''^2}\right)}{y}; \tag{3}$$

$$\bar{\rho}\tilde{u}\frac{\partial\tilde{H}}{\partial x}+\bar{\rho}\tilde{v}\frac{\partial\tilde{H}}{\partial y}=-\frac{\partial}{\partial x}\left(\bar{\rho}\widetilde{u''\tilde{H}''}\right)-\frac{\partial}{\partial y}\left(\bar{\rho}\widetilde{v''\tilde{H}''}\right)-\frac{\bar{\rho}\widetilde{v''\tilde{H}''}}{y}; \tag{4}$$

$$\bar{\rho}\tilde{u}\frac{\partial\tilde{C}}{\partial x}+\bar{\rho}\tilde{v}\frac{\partial\tilde{C}}{\partial y}=-\frac{\partial}{\partial x}\left(\bar{\rho}\widetilde{u''C''}\right)-\frac{\partial}{\partial y}\left(\bar{\rho}\widetilde{v''C''}\right)-\frac{\bar{\rho}\widetilde{v''C''}}{y}; \tag{5}$$

$$\tilde{H}=\int_0^{\tilde{T}}C_p dT+0.5\left(\tilde{u}^2+\tilde{v}^2\right)+K,\quad \bar{p}=\bar{\rho}R\tilde{T}/M_\Sigma. \tag{6}$$

where (x, y) is the orthogonal coordinate system (the x axis coincides with the axis of the jet); u, v are the axial and radial components of the velocity; ρ is the density; p is the pressure; H is the specific total enthalpy; C is the mass fraction of the inert component; R is the universal gas constant; M_Σ is the molecular mass of the gas mixture; C_p is the specific heat capacity at a constant pressure; T is the temperature.

To close the system, it is necessary to use some kind of a turbulence model. In this paper, we use a modification of the K–ε turbulence model, which takes into account the effect of high-speed compressibility on the turbulence intensity and also shows the best agreement with experiment on the calculation of turbulent jets [8, 9].

This model includes the following equations for K and ε:

$$\bar{\rho}\tilde{u}\frac{\partial K}{\partial x}+\bar{\rho}\tilde{v}\frac{\partial K}{\partial y}=-\frac{\partial}{\partial x}\left(\bar{\rho}\widetilde{u''K}\right)-\frac{\partial}{\partial y}\left(\bar{\rho}\widetilde{v''K}\right)-\frac{\bar{\rho}\widetilde{v''K}}{y}+P-\bar{\rho}\varepsilon+\kappa; \tag{7}$$

$$\bar{\rho}\tilde{u}\frac{\partial\varepsilon}{\partial x}+\bar{\rho}\tilde{v}\frac{\partial\varepsilon}{\partial y}=-\frac{\partial}{\partial x}\left(\bar{\rho}\widetilde{u''\varepsilon}\right)-\frac{\partial}{\partial y}\left(\bar{\rho}\widetilde{v''\varepsilon}\right)-\frac{\bar{\rho}\widetilde{v''\varepsilon}}{y}+\frac{\varepsilon}{K}\left(C_{\varepsilon1}P-C_{\varepsilon2}\bar{\rho}\varepsilon\right); \tag{8}$$

where $P=-\bar{\rho}\left[\widetilde{u''^2}\frac{\partial\tilde{u}}{\partial x}+\widetilde{u''v''}\left(\frac{\partial\tilde{u}}{\partial y}+\frac{\partial\tilde{v}}{\partial x}\right)+\widetilde{v''^2}\frac{\partial\tilde{v}}{\partial y}+\frac{\widetilde{w''^2}\tilde{v}}{y}\right]$, $\kappa=\overline{p'\frac{\partial u_i''}{\partial x_i}}$.

Here K is the turbulence kinetic energy; ε is the rate of turbulence dissipation; P is the generation of the turbulent energy.

For the coefficient of turbulent viscosity and for the pressure–divergence correlation, the following formulas are used [9]:

$$\mu_T=\frac{C_\mu}{1+0.29\,\mathrm{M}_T}\frac{\bar{\rho}K^2}{\varepsilon},\quad \kappa=-0.29\,\mathrm{M}_T, \tag{9}$$

where $\mathrm{M}_T=\sqrt{2K}/a$ is the turbulent Mach number; a is the sound speed.

The model uses the following numerical constants $C_\mu=0.09$; $C_{\varepsilon1}=1.44$; $C_{\varepsilon2}=1.92$.

As already indicated, this model is valid only for flows with high Reynolds numbers, because at lower numbers, it is necessary to take into account a molecular transport in system (1)–(5), and corrections for laminarization in equation (8).

Parabolization of the original differential equations is done by discarding some of the viscous terms included in these equations. It is believed that their influence can be neglected.

Usually, this discarding is carried out after the transition to a new coordinate system that transforms the real geometry of the computational domain into the rectangular one [5, 6]. It is clear that in this case the system to be solved and, accordingly, the result of the calculations depends on how this coordinate transformation will be performed. That is, a grid-dependent solution is obtained. In this work, a different approach was used, which was based only on the analysis of the physics of turbulent mixing processes.

First of all, let us consider θ (the inclination angle of the flow in the middle of the mixing layer with respect to the x axis) and also introduce an "oriented to the mixing layer" orthogonal coordinate system (s, n).

For viscous terms, it is assumed that

$$\frac{\partial}{\partial s} \ll \frac{\partial}{\partial n}, \quad V_s \gg V_n . \tag{10}$$

It follows from (10) that

$$\frac{\partial f}{\partial x} = \frac{\partial f}{\partial s}\cos\theta + \frac{\partial f}{\partial n}\sin\theta \approx \frac{\partial f}{\partial n}\sin\theta, \quad \frac{\partial f}{\partial y} = -\frac{\partial f}{\partial s}\sin\theta + \frac{\partial f}{\partial n}\cos\theta \approx \frac{\partial f}{\partial n}\cos\theta, \tag{11}$$

where f is any parameter included in the viscous terms of the system.

First, let us consider the scalar quantity transport equation (5). We use the assumptions about the gradient law for turbulent diffusion:

$$\bar{\rho}\widetilde{\mathbf{V}''C''} = -\frac{\mu_T}{\mathrm{Sc}_T}\nabla\tilde{C} \tag{12}$$

Then, taking into account (11), it is valid for the viscous terms on the right-hand side of Eq. (5)

$$-\nabla\left(\bar{\rho}\widetilde{\mathbf{V}''C''}\right) = \nabla\left(\frac{\mu_T}{\mathrm{Sc}_T}\nabla C\right) \approx \frac{1}{y}\frac{\partial}{\partial n}\left(y\frac{\mu_T}{\mathrm{Sc}_T}\frac{\partial C}{\partial n}\right) \approx \frac{1}{y}\frac{\partial}{\partial y}\left(y\frac{1}{\cos^2\theta}\frac{\mu_T}{\mathrm{Sc}_T}\frac{\partial C}{\partial y}\right). \tag{13}$$

It should be taken into account here that the angle θ is independent on the y coordinate. Sc_T is the turbulent Schmidt number. Similar transformations are valid for all transport equations of scalar values.

It was shown in [10] that in the components of momentum equation (2) and (3), the viscous terms can be represented as

$$\nabla\left(\mu_T\nabla u\right) + S_u, \quad \nabla\left(\frac{4}{3}\mu_T\nabla v\right) + S_v \tag{14}$$

and, neglecting the additional terms S_u, S_v, the formulas similar to (13) can be used for them.

As a result, we obtain the following system of equations describing turbulent axisymmetric gas jets:

$$\begin{gathered}
\frac{\partial}{\partial x}\left(\bar{\rho}\tilde{u}\right) + \frac{\partial}{\partial y}\left(\bar{\rho}\tilde{v}\right) + \frac{\bar{\rho}\tilde{v}}{y} = 0; \quad \bar{\rho}\tilde{u}\frac{\partial\tilde{u}}{\partial x} + \bar{\rho}\tilde{v}\frac{\partial\tilde{u}}{\partial y} = -\frac{\partial\bar{p}}{\partial x} + \frac{1}{y}\frac{\partial}{\partial y}\left(y\frac{1}{\cos^2\theta}\mu_T\frac{\partial\tilde{u}}{\partial y}\right); \\
\bar{\rho}\tilde{u}\frac{\partial\tilde{v}}{\partial x} + \bar{\rho}\tilde{v}\frac{\partial\tilde{v}}{\partial y} = -\frac{\partial\bar{p}}{\partial y} + \frac{\partial}{\partial y}\left(\frac{4}{3}\frac{1}{\cos^2\theta}\mu_T\frac{\partial\tilde{v}}{\partial y}\right); \quad \bar{\rho}\tilde{u}\frac{\partial C}{\partial x} + \bar{\rho}\tilde{v}\frac{\partial C}{\partial y} = \frac{1}{y}\frac{\partial}{\partial y}\left(y\frac{1}{\cos^2\theta}\frac{\mu_T}{\mathrm{Sc}_T}\frac{\partial C}{\partial y}\right); \\
\bar{\rho}\tilde{u}\frac{\partial\tilde{H}}{\partial x} + \bar{\rho}\tilde{v}\frac{\partial\tilde{H}}{\partial y} = \frac{1}{y}\frac{\partial}{\partial y}\left[y\frac{1}{\cos^2\theta}\mu_T\left(\frac{1}{\mathrm{Pr}_T}\frac{\partial\tilde{h}}{\partial y} + \frac{\partial K}{\partial y} + \frac{\tilde{u}}{\cos^2\theta}\frac{\partial\tilde{u}}{\partial y}\right)\right]; \\
\bar{\rho}\tilde{u}\frac{\partial K}{\partial x} + \bar{\rho}\tilde{v}\frac{\partial K}{\partial y} = \frac{1}{y}\frac{\partial}{\partial y}\left(y\frac{1}{\cos^2\theta}\mu_T\frac{\partial K}{\partial y}\right) + P - \bar{\rho}\varepsilon + \kappa; \\
\bar{\rho}\tilde{u}\frac{\partial\varepsilon}{\partial x} + \bar{\rho}\tilde{v}\frac{\partial\varepsilon}{\partial y} = \frac{1}{y}\frac{\partial}{\partial y}\left(y\frac{1}{\cos^2\theta}\frac{\mu_T}{\sigma_\varepsilon}\frac{\partial\varepsilon}{\partial y}\right) + \frac{\varepsilon}{K}\left(C_{\varepsilon 1}P - C_{\varepsilon 2}\bar{\rho}\varepsilon + \kappa\right).
\end{gathered} \tag{15}$$

Turbulent energy production is described by the formula $P = \frac{\mu_T}{\cos^4\theta}\left(\frac{\partial \tilde{u}}{\partial y}\right)^2$, and the numerical constants $\mathrm{Pr}_T = \mathrm{Sc}_T = 0.7$, $\sigma_\varepsilon = 1.3$ are assumed.

It should be noted that parabolized equations in the form of (15) can be used only for supersonic flows. The issue of calculating jets with subsonic regions is considered further.

System of equations (15) in a conservative form has the following vector form

$$\frac{\partial \mathbf{F}}{\partial x} + \frac{\partial \mathbf{G}}{\partial y} + \mathbf{H} = \mathbf{Y}^{-1}\frac{\partial}{\partial y}\left(\mathbf{YL}\frac{\partial \boldsymbol{\psi}}{\partial y}\right) + \mathbf{S}, \tag{16}$$

where

$$\mathbf{F} = \left(\rho u, \rho u^2 + p, \rho uv, \rho uH, \rho uC, \rho u\varepsilon, \rho uK\right)^T;$$

$$\mathbf{G} = \left(\rho v, \rho uv, \rho v^2 + p, \rho vH, \rho vC, \rho v\varepsilon, \rho vK\right)^T;$$

$$\mathbf{H} = \frac{1}{y}\left(\rho v, \rho uv, \rho v^2, \rho vH, \rho vC, \rho v\varepsilon, \rho vK\right)^T;$$

$$\boldsymbol{\psi} = \left(\rho, u, v, h, C, \varepsilon, K\right)^T;$$

$$\mathbf{Y} = \begin{pmatrix} 1 & 0 & 0 & 0 & 0 & 0 & 0 \\ 0 & \bar{y} & 0 & 0 & 0 & 0 & 0 \\ 0 & 0 & 1 & 0 & 0 & 0 & 0 \\ 0 & 0 & 0 & \bar{y} & 0 & 0 & 0 \\ 0 & 0 & 0 & 0 & \bar{y} & 0 & 0 \\ 0 & 0 & 0 & 0 & 0 & \bar{y} & 0 \\ 0 & 0 & 0 & 0 & 0 & 0 & \bar{y} \end{pmatrix}; \quad \mathbf{L} = \begin{pmatrix} 0 & 0 & 0 & 0 & 0 & 0 & 0 \\ 0 & \mu_T & 0 & 0 & 0 & 0 & 0 \\ 0 & 0 & \frac{4}{3}\mu_T & 0 & 0 & 0 & 0 \\ 0 & \frac{u\mu_T}{\cos^2\theta} & 0 & \mu_T/\mathrm{Pr}_T & 0 & 0 & \mu_T \\ 0 & 0 & 0 & 0 & \mu_T/\mathrm{Sc}_T & 0 & 0 \\ 0 & 0 & 0 & 0 & 0 & \mu_T/\sigma_\varepsilon & 0 \\ 0 & 0 & 0 & 0 & 0 & 0 & \mu_T \end{pmatrix}\frac{1}{\cos^2\theta};$$

$$\mathbf{S} = \left(0,0,0,0,0,\frac{\varepsilon}{K}\left(C_{\varepsilon 1}\rho \mathrm{P} - C_{\varepsilon 2}\rho\varepsilon + \pi_K + \kappa\right), \rho \mathrm{P} + \pi_K + \kappa - \rho\varepsilon\right)^T,$$

$\bar{y} = \frac{y}{R_a}$, R_a is the radius of the initial section of the jet. The averaging signs in these formulas are omitted.

The system is solved in a new coordinate system using a simple rectangular transformation:

$$\xi = \bar{x}, \quad \eta = \eta\left(\bar{x}, \bar{y}\right), \tag{17}$$

where $\bar{x} = \frac{x}{R_a}$.

The transpported form of Eq. (16) is

$$\frac{\partial \bar{\mathbf{F}}}{\partial \xi} + \frac{\partial \bar{\mathbf{G}}}{\partial \eta} + \bar{\mathbf{H}} = \mathbf{Y}^{-1}\frac{\partial}{\partial \eta}\left(\bar{\mathbf{L}}\frac{\partial \boldsymbol{\psi}}{\partial \eta}\right) + \bar{\mathbf{S}}, \tag{18}$$

where $\bar{\mathbf{F}} = \mathbf{F}/b$; $\bar{\mathbf{G}} = \mathbf{G} + \bar{a}\,\mathbf{F}/b$; $\bar{\mathbf{H}} = \mathbf{H}R_a/b$; $\bar{\mathbf{L}} = \mathbf{YL}b/R_a$; $\bar{\mathbf{S}} = \frac{\mathbf{S}R_a}{b}$; $\bar{a} = \frac{\partial \eta}{\partial \bar{x}}$; $b = \frac{\partial \eta}{\partial \bar{y}}$.

The splitting method [11] was applied to solve system (18). A special modification of the implicit MacCormack method is used to solve Eq. (18) without a source. For an inviscid case, it is presented in [12].

The predictor is presented as

$$\Delta\tilde{\mathbf{F}}_k^n = \Delta\xi\frac{\bar{\mathbf{G}}_k^n - \bar{\mathbf{G}}_{k+1}^n}{\Delta\eta} - \Delta\xi\bar{\mathbf{H}}_k^n + \left(\mathbf{Y}^{-1}\right)_k^n \frac{\Delta\xi}{2\Delta\eta^2}\left[\left(\bar{\mathbf{L}}_k^n + \bar{\mathbf{L}}_{k+1}^n\right)\left(\psi_{k+1}^n - \psi_k^n\right) - \left(\bar{\mathbf{L}}_k^n + \bar{\mathbf{L}}_{k-1}^n\right)\left(\psi_k^n - \psi_{k-1}^n\right)\right]; \tag{19}$$

$$\left(\mathbf{E} + \frac{\Delta\xi}{\Delta\eta}\left|\Omega\right|_k^n + \Delta\xi\left|\Phi\right|_k^n\right)\delta\tilde{\mathbf{F}}_k^{\overline{n+1}} = \Delta\tilde{\mathbf{F}}_k^n + \frac{\Delta\xi}{\Delta\eta}\left|\Omega\right|_{k+1}^n \delta\tilde{\mathbf{F}}_{k+1}^{\overline{n+1}}; \tag{20}$$

$$\tilde{\mathbf{F}}_k^{\overline{n+1}} = \tilde{\mathbf{F}}_k^n + \delta\tilde{\mathbf{F}}_k^{\overline{n+1}}. \tag{21}$$

The corrector is presented as

$$\begin{gathered}\Delta\tilde{\mathbf{F}}_k^{\overline{n+1}} = \Delta\xi\frac{\bar{\mathbf{G}}_{k-1}^{\overline{n+1}} - \bar{\mathbf{G}}_k^{\overline{n+1}}}{\Delta\eta} - \Delta\xi\bar{\mathbf{H}}_k^{\overline{n+1}} \\ +\Delta\xi\left(\mathbf{Y}^{-1}\right)_k^{n+1}\frac{1}{2\Delta\eta^2}\left[\left(\bar{\mathbf{L}}_k^{\overline{n+1}} + \bar{\mathbf{L}}_{k+1}^{\overline{n+1}}\right)\left(\psi_{k+1}^{\overline{n+1}} - \psi_k^{\overline{n+1}}\right) - \left(\bar{\mathbf{L}}_k^{\overline{n+1}} + \bar{\mathbf{L}}_{k-1}^{\overline{n+1}}\right)\left(\psi_k^{\overline{n+1}} - \psi_{k-1}^{\overline{n+1}}\right)\right];\end{gathered} \tag{22}$$

$$\left(\mathbf{E} + \frac{\Delta\xi}{\Delta\eta}\left|\mathbf{\Omega}\right|_k^{\overline{n+1}} + \Delta\xi\left|\mathbf{\Phi}\right|_k^{\overline{n+1}}\right)\delta\tilde{\mathbf{F}}_k^{n+1} = \Delta\tilde{\mathbf{F}}_k^{\overline{n+1}} + \frac{\Delta\xi}{\Delta\eta}\left|\mathbf{\Omega}\right|_{k-1}^{\overline{n+1}}\delta\tilde{\mathbf{F}}_{k-1}^{n+1}; \tag{23}$$

$$\tilde{\mathbf{F}}_k^{n+1} = \frac{1}{2}\left(\tilde{\mathbf{F}}_k^n + \tilde{\mathbf{F}}_k^{\overline{n+1}} + \delta\tilde{\mathbf{F}}_k^{n+1}\right). \tag{24}$$

Here $\mathbf{E}$ is the identity matrix; the matrices $\left|\mathbf{\Omega}\right|$ and $\left|\mathbf{\Phi}\right|$ have positive eigenvalues and are associated with the Jacobi matrices $\mathbf{\Omega} = \frac{\partial\bar{\mathbf{G}}}{\partial\bar{\mathbf{F}}}$, $\mathbf{\Phi} = \frac{\partial\bar{\mathbf{H}}}{\partial\bar{\mathbf{F}}}$.

After each step, the physical variables $\rho, u, v, p, C, K, \varepsilon$ should be determined by the conservative variables $\tilde{\mathbf{F}}$.

Let us consider the definition $\left|\mathbf{\Omega}\right|$ and $\left|\mathbf{\Phi}\right|$ for supersonic regions.

The matrix $\left|\mathbf{\Omega}\right|$ is diagonalized as

$$\left|\mathbf{\Omega}\right| = \boldsymbol{\sigma}^{-1}\mathbf{D}\boldsymbol{\sigma}, \tag{25}$$

where $\boldsymbol{\sigma}^{-1}$ is the matrix of eigenvectors of $\mathbf{\Omega}$ and $\boldsymbol{\sigma}$ is the inverse matrix of $\boldsymbol{\sigma}^{-1}$; $\mathbf{D}$ is the diagonal matrix with the following elements:

$$d_j = \max\left\{0.5\left(\left|\omega\right|_j + \frac{2l}{\Delta\eta} - \frac{\Delta\eta}{\Delta\xi}\right), 0\right\}. \tag{26}$$

Here $\left|\omega\right|_j = \left|b\lambda_j + \bar{a}\right|$; $\lambda_{1,2,5,6,7} = v/u$; $\lambda_{3,4} = \left(uv \mp aw\right)/N$; $w = \sqrt{u^2 + v^2 - a^2}$; $N = u^2 - a^2$; $l = \frac{b^2\mu_T}{\rho R_a u N\cos^2\theta}\left[u^2\left(\gamma/\mathrm{Pr}_T + 1\right) - a^2/\mathrm{Pr}_T\right]$; γ is the specific heat.

The matrix $\boldsymbol{\sigma}^{-1}$ is defined as

$$\boldsymbol{\sigma}^{-1} = \begin{pmatrix} -\beta & 0 & 1 & 1 & 0 & 0 & 0 \\ 0 & \beta u & (uw + av)/w & (uw - av)/w & 0 & 0 & 0 \\ 0 & \beta v & (vw - au)/w & (vw + au)/w & 0 & 0 & 0 \\ b_{41} & b_{42} & H & H & 0 & 0 & 0 \\ 0 & 0 & C & C & 1 & 0 & 0 \\ 0 & 0 & \varepsilon & \varepsilon & 0 & 1 & 0 \\ 0 & 0 & K & K & 0 & 0 & 1 \end{pmatrix}, \tag{27}$$

where $b_{41} = 2a^2 - \beta(H - 2\alpha); b_{42} = a^2 + 2\alpha; H = h + \alpha; \alpha = \frac{1}{2}(u^2 + v^2), \beta = \gamma - 1$.

The effect of viscosity is taken into account only by adjusting the eigenvalues in matrix **D**.

The matrix $|\mathbf{\Phi}|$ is diagonal

$$|\mathbf{\Phi}| = \varphi\mathbf{E}, \quad \varphi = \max\{0.5z - 1/\Delta\xi, 0\}, \tag{28}$$

where

$$z = \frac{1}{\bar{y}}\left(\frac{|z_1| + \sqrt{z_1^2 - 4z_2}}{2}\right); \quad z_1 = \frac{(\gamma+1)uv}{N}; \quad z_2 = \frac{\gamma v^2}{N}.$$

The main advantage of this approach is that inversion of the matrices in the implicit part (Eqs. (20) and (23)) is reduced to fast operations, namely, double multiplication of the matrices and inversing the diagonal matrix.

To suppress oscillations in the region of shock waves, the fourth-order damping was introduced into the difference scheme [13].

To calculate flows with subsonic regions, the Vigneron technology [14] is most often used, this technology is based on dividing the vector **F** into two parts depending on the longitudinal Mach number values and gives good results in calculating supersonic flow around bodies, i.e. in the presence of small subsonic areas in the near-wall region [6, 13]. It is inconvenient for submerged jets, in which subsonic areas occupy a significant part of the flow.

The disadvantage of the Vigneron technology is the fact that the matrices included in the numerical scheme are significantly complicated. Therefore, a different approach was used to calculate subsonic areas in this paper.

In the subsonic areas, a non-conservative form of the basic equations was used, i.e. system (15) in its purest form.

The pressure is considered to be set. To solve the system, a numerical predictor–corrector scheme similar to (19)–(24) is used. The "supersonic" technique is combined with the "subsonic" one as follows.

In each jet section $\xi = \xi^n$, the boundary points of the difference grid *KU* and *KD* are determined (Fig. 1), at which the velocity $u < 1.2a$ (the point *KD* exists only in the presence of a subsonic region behind the Mach disk).

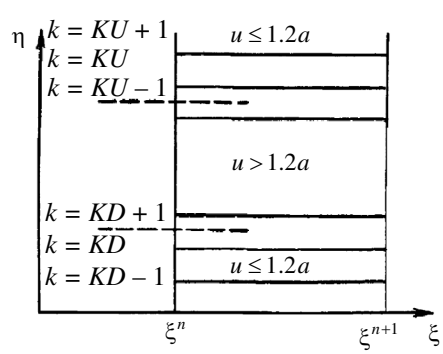

Fig. 1.

At the nodal points $k = 1, ..., KD$ and $k = KU, KU+1, ..., NN$, the calculation is carried out according to the "subsonic" technique (*NN* is the number of grid nodes). For $k = KD + 1, ..., KU - 1$, the "supersonic"

technique is used. In transition from the "subsonic" technique to the "supersonic" one at the nodes $k = KU$ and $k = KD$, the increments of the conservative vector $\delta\mathbf{F}$ are determined from the known values of the increments of the non-conservative vector; then they are used in the implicit part of the "supersonic" technique. Similarly, when switching from the "supersonic" technique to the "subsonic" one, at the nodes $k = KD + 1$ and $k = KU - 1$, the components of the non-conservative vector are determined from the given increments $\delta\mathbf{F}$. When using the predictor–corrector scheme, in which at each stage the transition is only down or only up the grid, this approach is very easily implemented.

An important issue is the determination of the pressure and the longitudinal derivative of pressure in the "subsonic" areas of the jet.

In the outer part of the jet, it is supposed that

$$p = p_E; \quad \frac{\partial p}{\partial x} = 0, \tag{29}$$

where p_E is the pressure of the external flow.

The technique described in detail in [11] was used for the region beyond the Mach disk.

The presented numerical method was applied to the calculation of jet flows.

The first test was devoted to testing the capabilities of the numerical method used and comparing it with the solution of the complete system of Navier–Stokes equations. For this, the air flow was calculated with the following parameters: $\mathrm{M}_a = 4$; $T_a = 2000$ K; $p_a / p_e = 10^5$; $\mathrm{M}_e = 12$; $T_e = 288$ K (here the subscript a refers to the parameters at the nozzle exit and the subscript e—to the parameters of the external flow).

This flow is characterized by the presence of regions with huge pressure gradients and very high Mach numbers. When using the shock-capturing calculation, the numerical solution is complicated.

Figure 2 shows the variation of pressure and density along the axis of the jet. The calculation results by the method of characteristics from [15] (dotted curve), the results when solving the complete Navier–Stokes system (solid curve), and the calculation results by the proposed technique (dash-dot curve) are compared.

Obviously, all calculations are in satisfactory agreement with each other. In addition, the calculation time when using parabolized equations is approximately two orders of magnitude shorter than for the solution of the complete system of Navier–Stokes equations. Some oscillations are observed in the region where the hanging shock and the reflected shock converge. This is explained by the fact that the subsonic region behind the Mach disk was not separately distinguished in this calculation. Because this area is very small in this case, such a simplification practically does not affect the calculation results.

The second test also focuses on comparing calculation results using the complete and parabolized system of Navier–Stokes equations.

A jet with the following parameters was used as the test case. Parameters at the nozzle exit: velocity—2900 m/s; pressure—0.75×10^5 Pa; temperature—1900K; outlet angle—0.17453 rad; radius—1 m. Composition, mole fractions: O_2—0.1631E–5; CO—0.08372; H—0.2406E–3; O—0.5037E–6; OH—0.1521E–3; NO—0.1058E–4; H_2—0.05415; H_2O—0.4053; CO_2—0.1461. The external flow velocity is 845 m/s.

Figure 3 shows the axial temperature variation. Here (*1*)—the calculation using the complete system of Navier–Stokes equations; (*2*)—the calculation using the parabolized system of Navier–Stokes equations.

The calculation results for these two techniques are very close; and again, there is some discrepancy behind the Mach disk. We used the kinetics of chemical combustion reactions described in [16].

The following tests are devoted to calculating submerged jets. As already mentioned, quite significant areas of the flow are subsonic in this case. The method presented in this paper was used in all calculations.

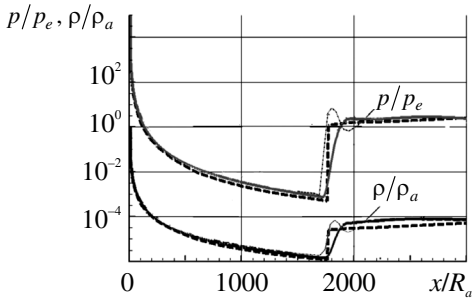

Fig. 2.

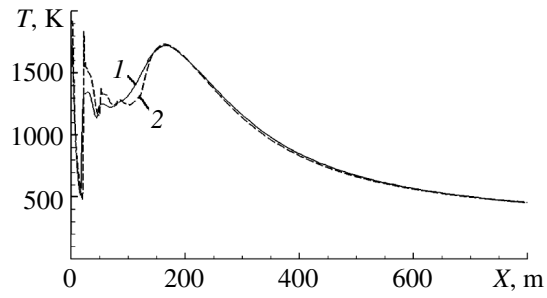

Fig. 3.

Figure 4 shows the dependence of the length of the submerged jet $\overline{X}_{0.75}$ on the Mach number at the nozzle exit. The calculation results are compared with experimental data. Here o—the experiment [17]; ▽—the experiment [18]; ▼—the experiment [19]; (*1*)—calculation using the *K*–ε model that includes the correction for compressibility [20]; (*2*)—calculation using the model of turbulence from [9].

As an estimate of the jet size, we used the dimensionless coordinate $\overline{X}_{0.75}$, at which the axial velocity u_C decreases to the value $0.75u_a$, i.e. it is 75% of the velocity on the nozzle exit axis.

Both models are in satisfactory agreement with experimental data and with each other, and also show an increase in jet length as the Mach number increases. When using the standard *K*–ε turbulence model, an increase in the estimated jet length with an increase in the Mach number is not observed.

Figure 5 shows the distribution of excess dimensionless Pitot pressure along the axis of the jet, having the following parameters: $T_0 = 2860$ K; $\mathrm{M}_a = 4.0$; $p_a/p_e = 0.65$. Here (*1*)—the experiment [21]; (*2*)—the calculation using the standard *K*–ε turbulence model; (*3*)—the calculation using the compressibility corrected *K*–ε model of turbulence [9]; (*4*)—the calculation using the compressibility corrected *K*–ε turbulence model [20].

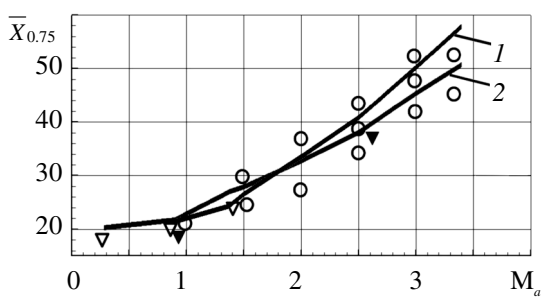

Fig. 4.

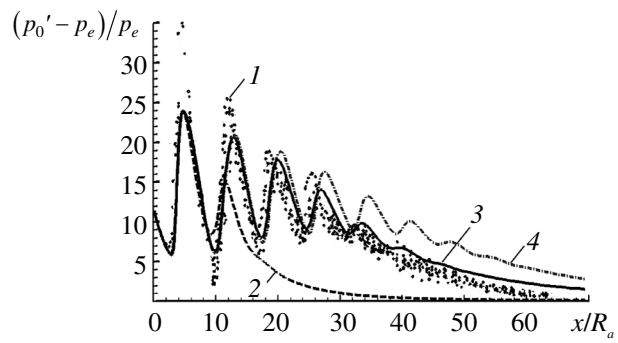

Fig. 5.

The calculation results for the turbulence model presented in this paper are in satisfactory agreement with the experiment, the standard *K*–ε turbulence model significantly underestimates the jet length; the *K*–ε turbulence model corrected by compressibility [20] somewhat overestimates the estimated jet length.

A modification of the implicit MacCormack method for calculating supersonic jets based on the parabolized Navier–Stokes equations is developed. The results obtained by this method are in fairly close agreement with the results of calculations based on the other methods and experimental data.

ACKNOWLEDGEMENTS

This work was supported by the Ministry of Education and Science of the Russian Federation, project no. 13.7418.2017/8.9.

REFERENCES

1. Fu Debin, Yu Yong, and Niu Qinglin, Simulation of Underexpanded Supersonic Jet Flows with Chemical Reactions, *Chinese Journal of Aeronautics*, 2014, vol. 27, no. 3, pp. 505–513.
2. Garaev, K.G., Derivation of the Prandtl–Sirazetdinov Equations for Optimally Controlled Boundary Layer Based on the Navier–Stokes Equations, *Izv. Vuz. Av. Tekhnika*, 2007, vol. 50, no. 2, pp. 12–13 [Russian Aeronautics (Engl. Transl.), vol. 50, no. 2, pp. 129–132].
3. Rodriguez, D., Sinha, A., Brès, G.A., and Colonius, T., Parabolized Stability Equation Models in Turbulent Supersonic Jets, *Proc. of the 18th AIAA/CEAS Aeroacoustics Conference*, 2012, Colorado Springs, USA, AIAA Paper 2012-2117.
4. Paredes, P. and Theofilis, V., Accurate Parabolic Navier–Stokes Solutions of the Supersonic Flow around an Elliptic Cone, 2013, *Proc. of the 51st AIAA Aerospace Sciences Meeting*, At Grapevine, TX, USA, AIAA Paper 2013-0670.
5. Williams, M., Edwards, J., and Prince, S., Application of a Parabolized Navier–Stokes Solver to Some Problems in Hypersonic Propulsion Aerodynamics, *Proc. of the AIAA Atmospheric Flight Mechanics Conference and Exhibit*, 2001, Montreal, Canada, AIAA Paper 2001-4066.
6. Lawrence, S.L., Tannehill, J.C., and Chaussee, D.S., Upwind Algorithm for the Parabolized Navier–Stokes Equations, *AIAA Journal*, 1989, vol. 27, no. 9. pp. 1175–1183.
7. MacCormack, R.W., A Numerical Method for Solving the Equations of Compressible Viscous Flow, *AIAA Journal*, 1982, vol. 20, no. 9, pp. 1275–1281.
8. Glebov, G.A. and Molchanov, A.M., Model of Turbulence for Supersonic Reacting Jets, *Issledovanie teploobmena v letatelnykh apparatakh* (Investigation of Heat Transfer in Flying Vehicles), Moscow: MAI, 1982, pp. 6–11.
9. Molchanov, A.M., A Calculation of Supersonic Non-Isobaric Jets with Compressibility Corrections in a Turbulence Model, *Vestnik MAI*, 2009, vol. 16, no. 1, pp. 38–48.
10. Molchanov, A.M., *Matematicheskoe modelirovanie zadach gazodinamiki i teplomassoobmena* (Mathematical Modeling of Gas Dynamics and Heat and Mass Transfer Problems), Moscow: MAI, 2013.
11. Molchanov, A.M. Calculation of Turbulent Supersonic Jets of Real Gas Flowing into Submerged Space, *Vestnik MAI*, 1997, vol. 4, no. 1, pp. 58–64.
12. Molchanov, A.M., Numerical Method for Supersonic Nonisobaric Jet Calculation, *Izv. Vuz. Av. Tekhnika*, 1989, vol. 32, no. 3, pp. 42–44 [Soviet Aeronautics (Engl. Transl.), vol. 32, no. 3, pp. 45–48].
13. Lawrence, S.L., Chaussee, D.S., and Tannehill, J.C., Application of the Implicit MacCormack Scheme to the Parabolized Navier–Stokes Equations, *AIAA Journal*, 1984, vol. 22, issue 12, pp. 1755–1763.
14. Vigneron, Y.C., Rakich, J.V., and Tannehill, J.C., Calculation of Supersonic Viscous Flow over Delta Wings with Harp Subsonic Leading Edges, *Proc. of the 11th Fluid and Plasma Dynamics Conference,* 1978, Seattle, AIAA Paper 78-1137.
15. Averenkova, G.I., Ashratov, E.A., Volkonskaya, T.G., et al. *Sverkhzvukovye strui ideal'nogo gaza* (Supersonic Jets of the Ideal Gas), Moscow: MGU, 1970.
16. Bykov, L.V., Molchanov, A.M., and Yanyshev, D.S., Numerical Method for Supersonic Turbulent Reacting Flow Simulations, *Vestnik MAI*, 2010, vol. 17, no. 3, pp. 108–119.
17. Krasotkin, V.S., Myshanov, A.I., Shalaev, S.P., Shirokov, N.N., and Yudelovich, M.Ya., Investigation of Supersonic Isobaric Submerged Turbulent Jets, *Izv. Akademii Nauk SSSR, Mekhanika Zhidkosti i Gaza*, 1988, vol. 23, no. 4, pp. 56–62 [Fluid Dynamics (Engl. Transl.), vol. 23, no. 4, pp. 529–534].
18. Lau, J.C., Morris, P.J., and Fisher, M.J., Measurements in Subsonic and Supersonic Free Jets using a Laser Velocimeter, *J. of Fluid Mechanics*, 1979, vol. 93, issue 1, pp. 1–27.
19. Glassman, I. and John, E.A.J. An Unusual Aerodynamic Stagnation-Temperature Effect, *J. of the Aerospace Sciences*, 1959, vol. 26, issue 6, pp. 387–388.

20. Sarkar, S., Erlebacher, G., Hussaini, M.Y., and Kreiss, H.O., *The Analysis and Modeling of Dilatational Terms in Compressible Turbulence*, NASA Center: Langley Research Center, 1989, Report Number: ICASE-89-79, NAS 1.26:181959, NASA-CR-181959.
21. Safronov, A.V., The Method of Calculation of the Jets of Combustion Products at the Rocket Launch, *Fiziko-khimicheskaya kinetika v gazovoi dinamike*, 2006, vol. 4, pp. 350–368.